AD-A035 674

ANALYSIS OF THE FRICTION BEHAVIOR AT HIGH SLIDING VELOCITIES AND PRESSURES FOR GLIDING METAL, ANNEALED IRON, COPPER AND PROJECTILE STEEL

BALLISTIC RESEARCH LABORATORIES
ABERDEEN PROVING GROUND, MARYLAND

JANUARY 1977

BRL

AD

REPORT NO. 1955

ANALYSIS OF THE FRICTION BEHAVIOR AT HIGH SLIDING VELOCITIES AND PRESSURES FOR GILDING METAL, ANNEALED IRON, COPPER AND PROJECTILE STEEL

James O. Pilcher, II
Emma M. Wineholt

January 1977

Approved for public release; distribution unlimited.

USA BALLISTIC RESEARCH LABORATORIES
ABERDEEN PROVING GROUND, MARYLAND

Destroy this report when it is no longer needed.
Do not return it to the originator.

Secondary distribution of this report by originating or sponsoring activity is prohibited.

Additional copies of this report may be obtained from the National Technical Information Service, U.S. Department of Commerce, Springfield, Virginia 22151.

The findings in this report are not to be construed as an official Department of the Army position, unless so designated by other authorized documents.

UNCLASSIFIED

SECURITY CLASSIFICATION OF THIS PAGE (When Data Entered)

REPORT DOCUMENTATION PAGE		READ INSTRUCTIONS BEFORE COMPLETING FORM
1. REPORT NUMBER REPORT NO. 1955	2. GOVT ACCESSION NO.	3. RECIPIENT'S CATALOG NUMBER
4. TITLE (and Subtitle) Analysis of the Friction Behavior at High Sliding Velocities and Pressures for Gilding Metal, Annealed Iron, Copper and Projectile Steel		5. TYPE OF REPORT & PERIOD COVERED BRL Report 6. PERFORMING ORG. REPORT NUMBER
7. AUTHOR(s) James O. Pilcher, II Emma H. Wineholt		8. CONTRACT OR GRANT NUMBER(s)
9. PERFORMING ORGANIZATION NAME AND ADDRESS US Army Ballistic Research Laboratory Aberdeen Proving Ground, Maryland 21005		10. PROGRAM ELEMENT, PROJECT, TASK AREA & WORK UNIT NUMBERS 1X663606D006
11. CONTROLLING OFFICE NAME AND ADDRESS US Army Materiel Development and Readiness Command 5001 Eisenhower Avenue Alexandria, Virginia 22333		12. REPORT DATE JANUARY 1977 13. NUMBER OF PAGES 70
14. MONITORING AGENCY NAME & ADDRESS(if different from Controlling Office)		15. SECURITY CLASS. (of this report) UNCLASSIFIED 15a. DECLASSIFICATION/DOWNGRADING SCHEDULE

16. DISTRIBUTION STATEMENT (of this Report)

Approved for public release; distribution unlimited.

17. DISTRIBUTION STATEMENT (of the abstract entered in Block 20, if different from Report)

18. SUPPLEMENTARY NOTES

A paper of the same title was presented to the TTCP Panel W2, 8 July 1976, Monterey, California.

19. KEY WORDS (Continue on reverse side if necessary and identify by block number)

friction	numerical data
high pressure	elastic-plastic slider
high velocity	dimensional analysis
properties of gilding metal	self-lubrication
properties of annealed iron	

20. ABSTRACT (Continue on reverse side if necessary and identify by block number) (cee)

Through the numerical analyses of the data presented in the Benet Weapons Laboratory Report No. WVT-TR-75028, "Friction and Wear at High Sliding Speeds," and dimensional analysis incorporating findings of Prandtl, Grosch and Plake, Bowden, Archard and W.R.D. Wilson, a formulation is developed equating the coefficient of friction to the normal pressure, sliding velocity, strength and thermodynamical properties of the slider. This equation is for an elastic-plastic slider sliding on a dry, rigid surface similar to the conditions in interior ballistic environments.

DD FORM 1 JAN 73 1473 EDITION OF 1 NOV 65 IS OBSOLETE

UNCLASSIFIED

SECURITY CLASSIFICATION OF THIS PAGE (When Data Entered)

TABLE OF CONTENTS

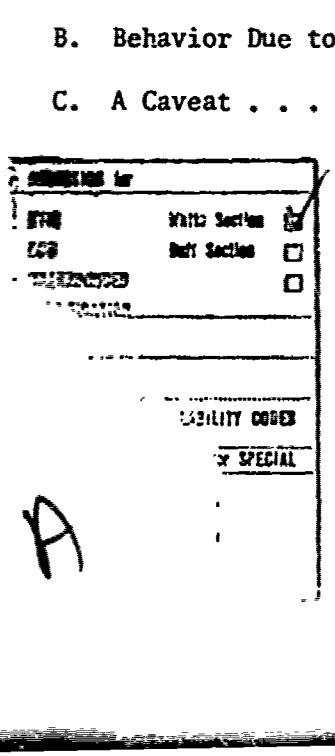

TABLE OF CONTENTS (Cont'd)

LIST OF ILLUSTRATIONS

I. INTRODUCTION

The understanding of the frictional behavior of dry sliding surfaces under dynamic conditions is essential to the prediction of interior ballistic performance of cannon systems. An accurate interior ballistic model of a cannon system not only requires an accurate description of the propellant and combustion processes but also necessitates reasonable descriptions of the mechanical response of the projectile, tube and recoil system and the forces generated at the interfaces of these system components. These interfaces contain surfaces which are subjected to a wide range of loadings and relative velocities. These surface loadings cause forces which must be considered in interior ballistic calculations, but which are difficult to mathematically model accurately.

Two examples of interior ballistic interfaces are the resistance of a projectile sliding through the tube and the surface traction between component parts of a saboted projectile. Modeling the first interface requires a knowledge of the frictional behavior for high bearing pressure (approximately twice the yield strength of the material) over a wide range of velocity (0 to 1500 m/s). Modeling the second interface requires an understanding of the frictional behavior for low velocities over a wide range of varying pressure (0 to the yield strength of the material). In both cases, the pressure and velocity conditions far exceed the conditions normally expected in the design of machinery components. This makes the formulations and values cited in most general engineering texts and handbooks inadequate for these types of problems.

The classical theory as well as various modern theories of friction are based on observations for relatively narrow ranges of pressure and velocity variations. The specificity of these laws precludes their use as a general treatment of frictional behavior over the range of pressures and velocities experienced in interior ballistic environments.

This report presents an analytical extrapolation and interpretation of friction data which were taken from an extensive experimental study performed for the Army by the Franklin Institute from about 1946 to 1956. These data recently collected and presented by Dr. R. S. Montgomery of Watervliet Arsenal represent, in the opinion of the authors, the best single collection of friction data over wide ranges of velocity and pressure.

The analysis discussed in this report was performed by the Ballistic Research Laboratories as part of the M483 Sticker Investigation Program for the Program Manager - Selected Ammunition.

II. EXPERIMENTAL DATA

The prime source of friction data examined in this analysis is taken from R. S. Montgomery's report,[1] "Friction and Wear at High Sliding Speeds", which summarizes the Franklin Institute experiments. These experiments were conducted for the Army from 1946 to 1956 and, due to their security classification (which has since been downgraded) and extremely limited distribution, these data were forgotten. Montgomery's report represents the first exposure of any consequence for these data.

A. The Franklin Institute Experiments

These experiments consisted of two small pins of specimen material in contact with opposite sides of a 61cm diameter rotating disc of gun steel. The frictional and normal forces were measured continuously by means of strain gages in the pin holders. The pins were made to follow non-overlapping spiral paths across the faces of the disc so that fresh disc surfaces were always presented to the pins during the experiments. Pins with 2.03mm diameter cross sections were used for the majority of the tests. Figure 1 shows the basic experimental arrangement. Table I gives the composition of the steel discs.

TABLE I. COMPOSITION OF STEEL TEST DISC

(% by weight)

Fe(%)	C(%)	Mn(%)	Ni(%)	Cr(%)	Mo(%)	V(%)	Si(%)	P(%)	S(%)
94.4	.35	.59	2.78	.98	.52	.12	.21	.022	.015

The data from these experiments are tabulated in the appendices according to material combinations; Appendix A for gilding metal on steel, Appendix B for soft iron on steel, Appendix C for copper on steel, and Appendix D for projectile steel on steel. Each appendix also contains the composition table for its respective pin material. Three variables are tabulated in the appendices, namely:

- P, the pressure normal to the sliding surface, in Pa
- V, the relative velocity between the two sliding members, in m/s
- μ, the coefficient of sliding friction, dimensionless

[1] *R. S. Montgomery, "Friction and Wear at High Sliding Speeds," Wear, Vol 36 (1976), pp 275-298.*

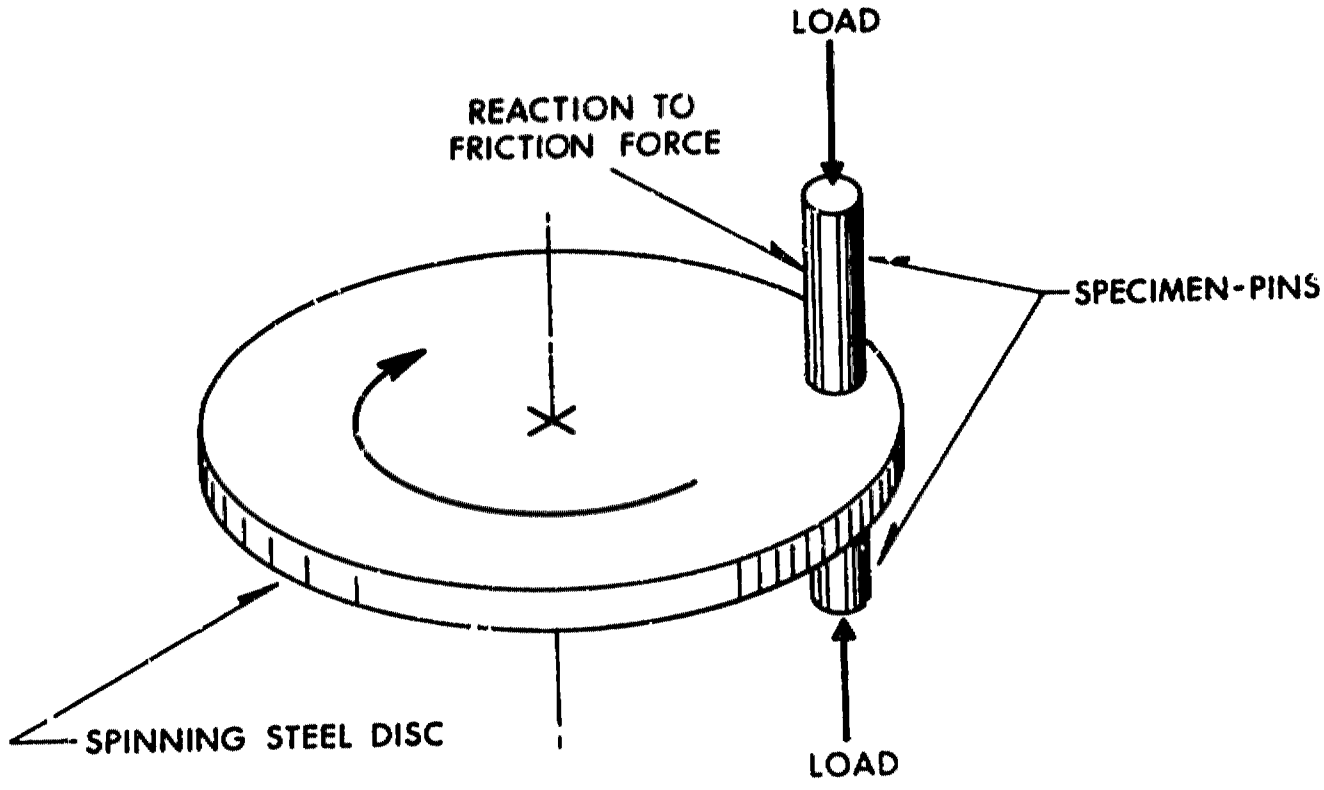

Figure 1. Schematic of the Experimental Configuration Used by the Franklin Institute.

The coefficient of friction, μ, is defined as the ratio of the resistance, F_r, to the normal force, PA, which is the product of the pressure, P, and contact area, A.

$$\mu = F_r/PA \tag{1}$$

B. Montgomery's Interpretation of the Franklin Institute Data

Montgomery attributes the frictional behavior of gilding metal, annealed iron, copper and projectile steel sliding on gun steel to the occurrence of surface melting due to the heat generated at the sliding surfaces. This interpretation is supported in part by the observed relationship between the coefficient of friction and the heat flux, Q, which is the triple product of the coefficient of friction, μ, normal pressure, P, and velocity, V.

$$\mu = f(Q) = f(\mu PV) \tag{2}$$

Figure 2 shows a plot of the coefficient of friction versus the heat flux for gilding metal. The data for annealed iron, copper and projectile steel follow the same pattern. The plot shows that, for increasing values of the heat flux, the coefficient of friction asymptotically approaches some function of heat flux. The plot also shows a rapidly increasing dispersion in the coefficient of friction with decreasing values of the heat flux. This dispersion is attributed by Montgomery to the unstable transition from a dry sliding surface to a completely wetted surface due to development of a molten film of the slider material. He also attributes dispersion to the difficulty of experimental control.

C. The Authors' Interpretation of the Franklin Institute Data

The trend of the data in Figure 2 indicates that, for values of heat flux above $3GW/m^2$, a function relating the coefficient of friction to the heat flux could be obtained. However, below $3GW/m^2$ of heat flux such a function would not be practicable. If the phenomena involved in the process were unstable on a macroscopic scale, then one would expect the data to show a steplike change in the coefficient of friction corresponding to an abrupt change of state of the contact surface (from solid to liquid phase and vice versa). Instead, the data exhibits a homogeneous distribution of values over the region. Certainly, the data do not exhibit bistability. From this it is evident that a function in terms of heat flux as the sole independent variable will not yield unique values of the coefficient of friction over the entire range of the data. Consequently, a different approach is required to further analyze the data.

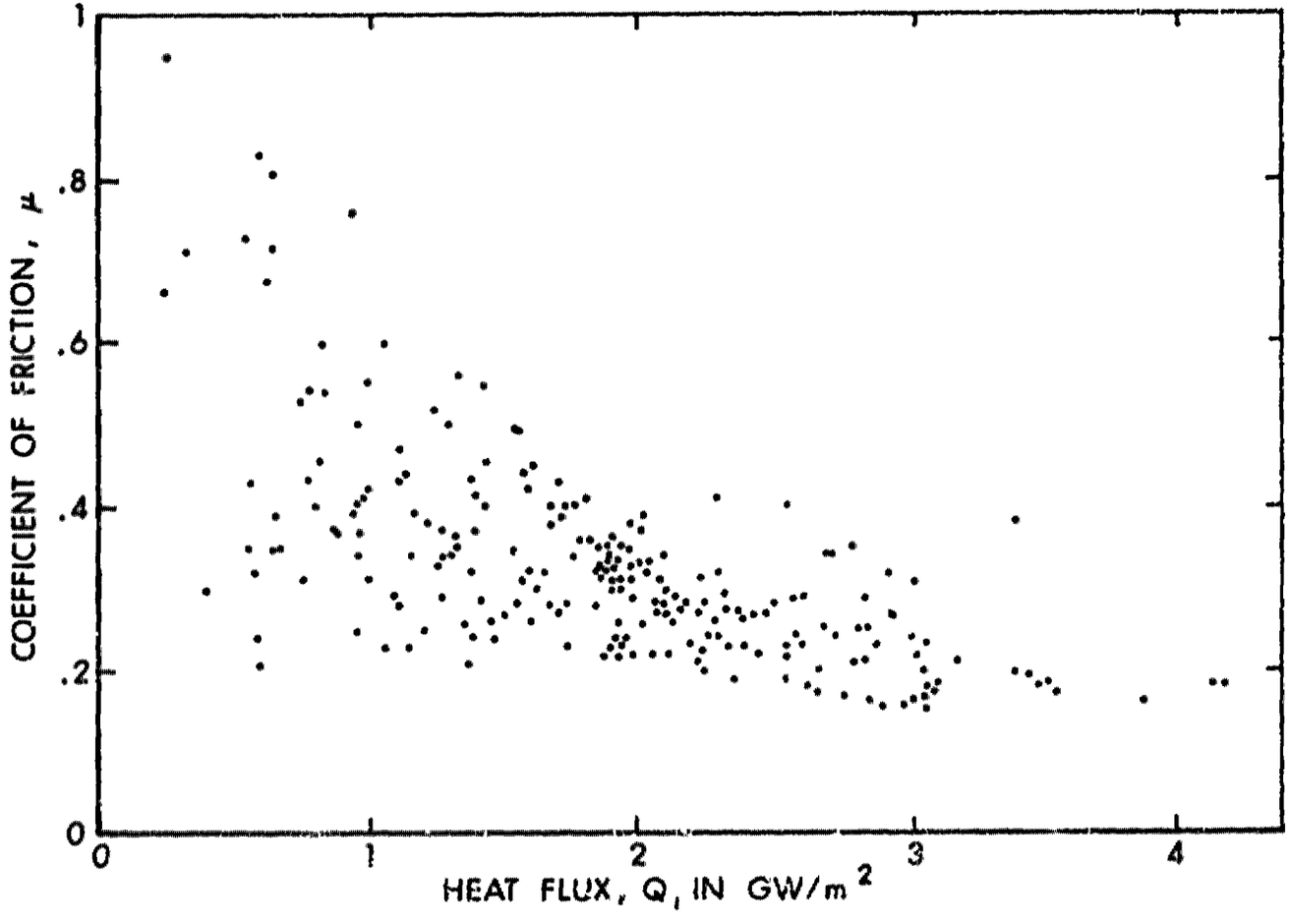

Figure 2. Coefficient of Friction Versus Heat Flux for Gilding Metal from Measurements by the Franklin Institute

The above interpretation is reinforced because the Buckingham Pi Theorem[2] indicates that equation (2) is incomplete.

III. NUMERICAL ANALYSIS OF THE FRANKLIN INSTITUTE FRICTION DATA

Based on the authors' previous interpretation of the data, the first basic assumption is that the coefficient of friction can be expressed as a function of the independent variables, V, P, and critical constants, μ_o, V_c, P_c.

$$\mu = f\ (\mu_o,\ V/V_c,\ P/P_c) \tag{3}$$

where μ_o is the static coefficient of friction
V is the sliding velocity
V_c is the critical sliding velocity, an intrinsic property of the material
P is the pressure across the sliding interface
P_c is the critical pressure across the interface, an intrinsic property of the material.

The coefficients μ_o, V_c and P_c are dependent on other variables such as geometry, temperature, and material strength properties. However, since these variables are held constant in the experiments, μ_o, V_c and P_c will be considered constants intrinsic to the materials and geometry used. These constants are chosen as a matter of convenience rather than for their specific physical meaning.

The second assumption is that the independent variables are separable. Historically, investigators have been able to experimentally separate the effects of load or pressure from velocity. This empirical evidence logically induces this assumption. Hence we can restate equation (3) as

$$\mu = \mu_o\ f\ (V/V_c)G\ (P/P_c) \tag{4}$$

Under this assumption the data can be separated into sets having commonalities, such as all points having the same velocity. The Franklin Institute experiments were run at constant velocities with varying pressures. The data are arranged according to velocity in the appendices.

---

[2] *W. E. Baker, P. S. Westine and F. T. Dodge, Similarity Methods in Engineering Dynamics, Hayden Book Company, Inc., Rochelle Park, NJ, 1973, Chapter 3.*

A. Pressure Effects

In analyzing the effects of pressure on frictional behavior, a literature review was made concerning the classical and modern friction laws to gain understanding of the problem. The most pertinent works examined were those of Amontons' in 1699,[3] Bowden in 1938,[4] and Archard in 1957.[5] A comparison of the relationships established by the investigators was made by taking the ratio of the friction force calculated from these relationships to the friction force for constant coefficient of friction. These ratios were calculated as a function of the ratio of normal pressure to critical pressure. The range of validity for each relationship was determined by the authors as the range of the respective published data and recast in normalized form. Based on the analysis of the Franklin Institute data the critical pressure was assumed to be approximately the yield strength of the material.

From equations (1) and (4)

$$\mu = CG\ (P/P_c) \tag{5}$$

and

$$F_r = CPAG\ (P/P_c) \tag{6}$$

and the critical static friction force F_c can be expressed as

$$F_c = CP_c\ A \tag{7}$$

where: C is a dimensionless constant of proportionality; P_c is the critical pressure, an intrinsic property of the material; F_c is the critical static friction force.

---

[3] *F. Palmer, "What About Friction," American Journal of Physics, 1949.*

[4] *F. P. Bowden and D. Tabor, Friction and Lubrication, John Wiley and Sons, Inc., New York, 1956.*

[5] *J. F. Archard, "Single Contacts and Multiple Encounters," Journal of Applied Physics, 1961, Vol 32.*

The ratio of F_r to F_c then becomes

$$F_{r/F_c} = \frac{P}{P_c} G\,(P/P_c) \tag{8}$$

From Amontons' Law (classical law) we have

$$\mu = c \tag{9}$$

and

$$F_{r/F_c} = P/P_c \tag{10}$$

Common engineering practice and experience place the range of validity for this law[6] at

$$0 < P/P_c < .025 \tag{11}$$

From Archard's law, we have

$$\mu = C \left[P/P_c\right]^{-1/3} \tag{12}$$

and

$$F_{r/F_c} = \left[P/P_c\right]^{2/3} \tag{13}$$

Based on his published data, Archard's relation is applicable for a pressure regime between

$$.025 < P/P_c \leq .4 \tag{14}$$

From Bowden's theory of friction which states that the actual contact area varies as a function of the total load, one can conclude that, in the elastic regime, on a macroscopic scale, some maximum area will be achieved along with some maximum pressure corresponding to the yield strength of the material. Increased loading would cause material flow which can aid sliding. In addition, localized

---

[6] *A. Gemant, Frictional Phenomena, Chemical Publishing Co., Inc, Brooklyn, NY 1950.*

changes of state of the material due to internal heat could cause the buildup of a fluid film, as observed by Montgomery and others. These reasonings suggest that a maximum in the friction force would occur about the point of incipient plastic flow.

Bowden states the coefficient of friction as the ratio of the shear strength to the yield strength of the material

$$\mu_o = s/y \tag{15}$$

where s is the shear strength of the material, and y is the yield strength of the material. If the sliding member is loaded near the yield stress of the material, one can expect localized strain-hardening of the material, particularly the elastic-plastic materials, causing a decrease in the coefficient of friction due to an increase in the effective yield stress of the material. This further indicates the existence of some maximum limiting friction force obtainable over the range of loads of interest.

To estimate the relative friction force, F_r/F_c, at the point of incipient flow of the material, the material is assumed to be strain-hardened homogeneously as the plastic state is reached. Although, in reality, a three-dimensional stress field exists, the Huber-Mises-Hencky[7] condition for plane stress was used to calculate the range of values that the coefficient of friction might achieve as defined by Bowden.

The Huber-Mises-Hencky condition for plane stress is

$$\left[S_1 + S_2\right]^2 + 4\, S_{12}^2 = 4\, S_o^2 /3 \tag{16}$$

where S_1, S_2 = the orthogonal stresses

S_{12} = the shear stress

S_o = yield stress

and $$S_2 = 0;\ S_1 = P;\ S_o = P_c;\ S_{12} = \mu P;\ P \rightarrow P_c$$

It can be shown that under these conditions equation (16) is satisfied when

$$\mu \rightarrow .29$$

$$\text{as } P \rightarrow P_c \tag{17}$$

---

[7] *A. M. Freudenthal.* *The Inelastic Behavior of Engineering Materials and Solid Structures*, *John Wiley and Sons, New York, 1950, page 261.*

The ratio of the friction force to the st tic equivalent is

$$F_r/F_c = \frac{\mu PA}{\mu_o P_c A} = \frac{.29}{\mu_o}$$

$$\text{as } P \rightarrow P_c \tag{18}$$

Since measurements by various investigators reported in the ASTM Metals Handbook indicate that values

$$.6 < \mu_o < 2. \tag{19}$$

can be expected for the materials under investigation; it can be expected that

$$.15 < F_r/F_c < .48$$

$$\text{at } P/P_c = 1 \tag{20}$$

Our knowledge of the effects of pressure on the coefficient of friction can be summarized in a plot showing a comparison of various laws over their respective regions of applicability, as shown in Figure 3. This plot shows the expected envelope in which a continuous relationship of the relative friction force, F_r/F_c, versus the relative normal pressure, P/P_c should exist. The desired function should describe the transition from one law to the other. The region denoted by the horizontal dashed lines indicates the domain and the range in which Bowden's law would apply.

Figure 4 shows a plot of the coefficient of friction versus normal pressure for gilding metal sliding on gun steel at 91.5 m/s. This plot is characteristic of all the sets of constant velocity data. Equation (4) can be restated as

$$\mu_i = a_i\, G(P) \tag{21}$$

where $V = V_i$; $a_i = \mu_o\, f(V_i)$

a_i is a dimensionless constant of proportionality corresponding to a constant velocity, V_i. μ_i is the coefficient of friction corresponding to V_i and P.

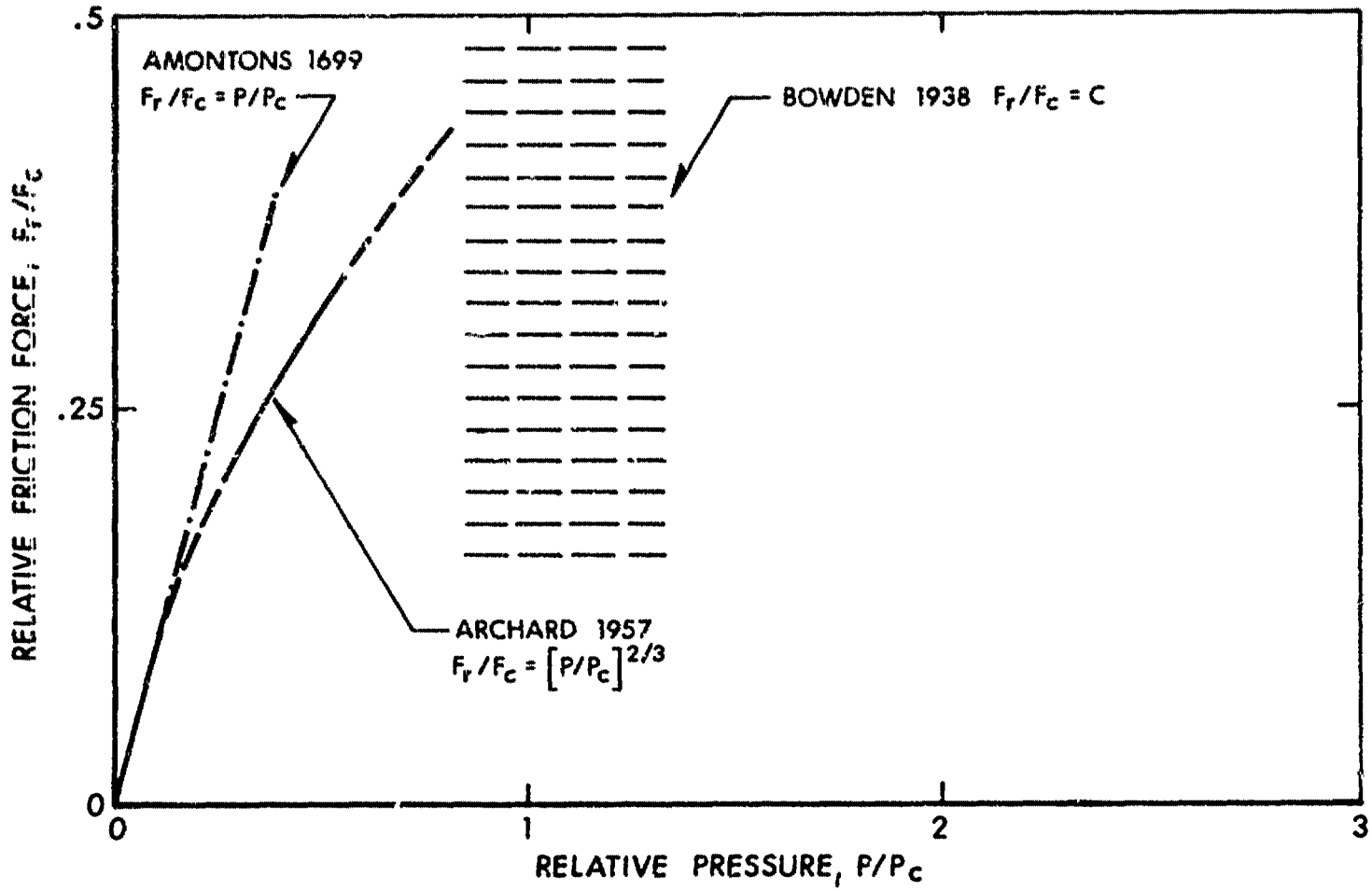

Figure 3. Plot Showing the Comparison of the Relative Friction Force to Relative Normal Pressure for Amontons, Bowden and Archard Laws.

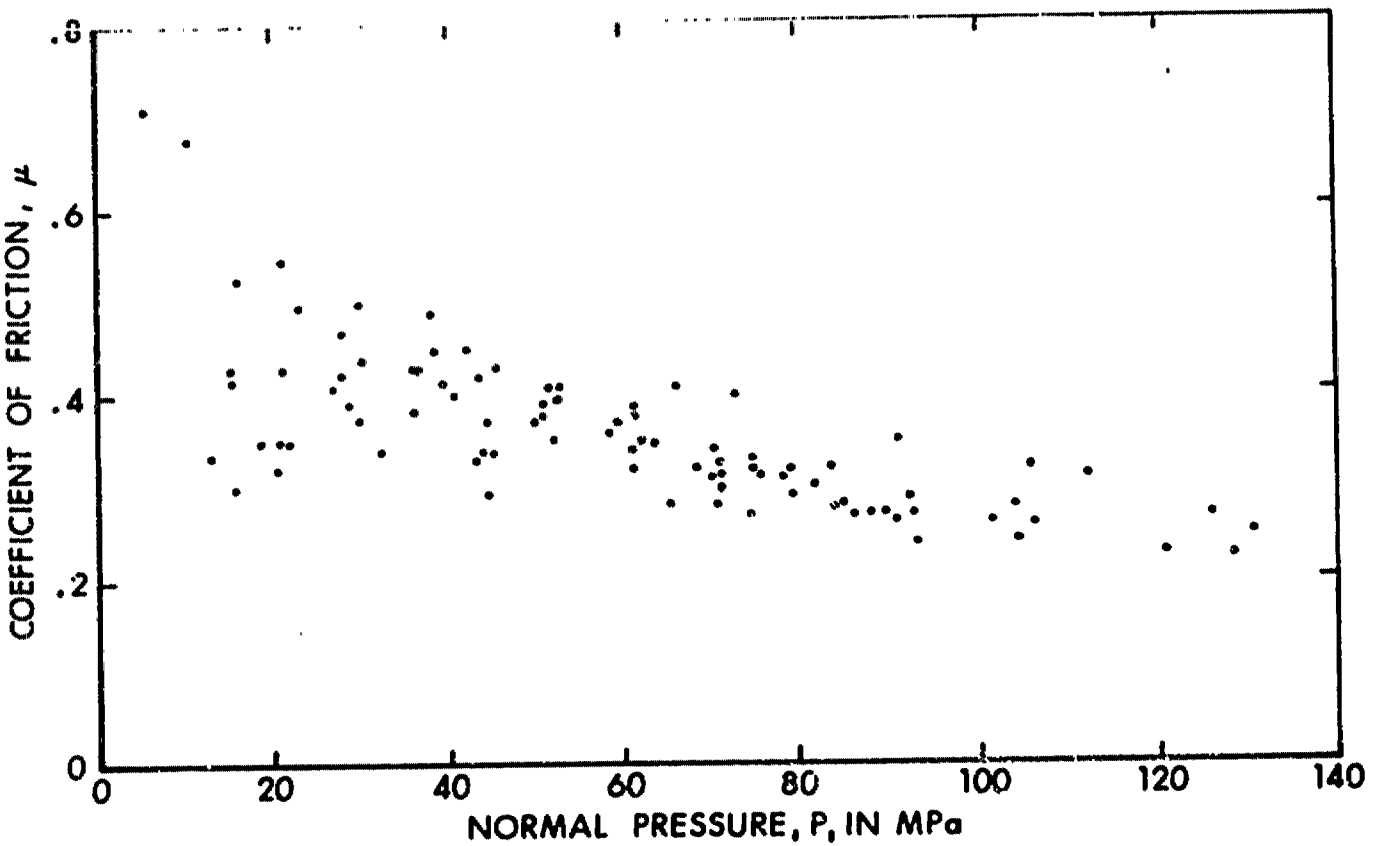

Figure 4. Plot Showing the Measured Values of the Coefficient of Friction Versus the Normal Pressure for Gilding Metal Sliding on Steel at a Constant Velocity of 91.5 m/s.

Since a least squares expansion finds a uniform approximation in an interval rather than about a point as in a power series expansion, each set of constant velocity data was analyzed by use of the Theory of Least Squares[8] to determine the best fitting of the following equation forms:

$$\text{a)}\quad \mu_i = a_i\,(b + cP + dP^2)$$

$$\text{b)}\quad \mu_i = a_i\left(\frac{1 + bP}{1 + cP}\right)$$

$$\text{c)}\quad \mu_i = a_i\,(P^b)$$

$$\text{d)}\quad \mu_i = a_i\,(e^{bP})$$

$$\text{e)}\quad \mu_i = a_i\left(\frac{1 + bP + cP^2}{1 + dP + hP^2}\right) \qquad (22)$$

The best fit was obtained by using an exponential form as shown in equation (22d). The residual differences from the mean of the data were two orders of magnitude better than those of any of the other forms at all velocities for all materials. Table II shows the values obtained for the constants a_i and b where

$$\mu_i = a_i e^{bP} \qquad (23)$$

for each of the materials tested.

Figure 5 shows a plot of equation (23) with its standard deviation superimposed over the data shown in Figure 4.

Since μ_i is dimensionless,

$$a_i e^{bP}$$

[8] *R. W. Hamming, Numerical Methods for Scientists and Engineers, McGraw-Hill, New York, 1962, pp 223-225.*

TABLE II. CALCULATED VALUES FOR a_i AND b AT VELOCITY V_j FOR GILDING METAL, ANNEALED IRON, COPPER AND PROJECTILE STEEL SLIDERS

Material	b, in MPa^{-1}	a_i	V_i, in m/s
Gilding Metal	-.0058 ± .0002	.74 ± .095	45.7
		.49 ± .059	91.5
		.39 ± .042	137.2
		.34 ± .026	182.9
		.23 ± .006	365.8
Annealed Iron	-.0049 ± .0004	.52 ± .043	45.7
		.45 ± .116	91.5
		.34 ± .031	137.2
		.31 ± .029	182.9
		.25 ± .017	274.3
Copper	-.0048 ± .0003	1.01 ± .170	45.7
		.38 ± .030	182.9
		.33 ± .031	274.3
		.30 ± .027	365.8
		.28 ± .023	457.2
Projectile Steel	-.0064 ± .0016	.42 ± .045	182.9
		.43 ± .037	274.3
		.42 ± .027	365.8

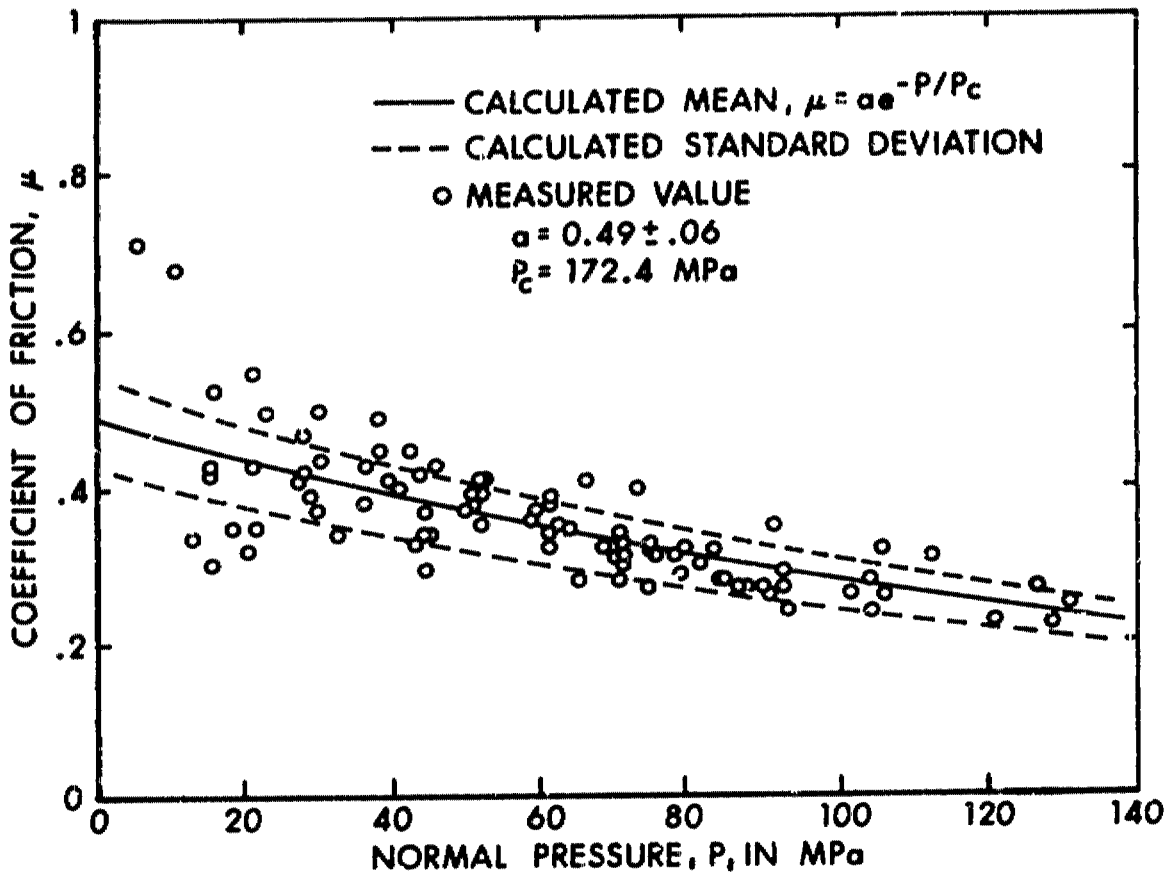

Figure 5. Plot Showing a Comparison of the Calculated to Measured Values of the Coefficient of Friction Versus Normal Pressure of Gilding Metal Sliding on Steel at a Constant Velocity 91.5 m/s.

must also be dimensionless. Based on the assumption of separability, a_i is assumed to be dimensionless; also, bP must be made dimensionless. From the analysis

$$-1 < b < 0 \tag{24}$$

therefore,

$$e^{bP} = e^{-P/P_c} \tag{25}$$

where $P_c = \frac{1}{|b|}$ is the critical pressure, a property of the weaker of the two materials.

Thus, in a nondimensionalized form

$$\mu_i = a_i e^{-P/P_c} \tag{26}$$

Table III shows the calculated critical pressure, P_c, for the materials tested.

TABLE III. CALCULATED CRITICAL PRESSURES FOR MATERIALS TESTED BY FRANKLIN INSTITUTE

Material	P_c, in MPa
Gilding Metal	172. ± 6.
Annealed Iron	204. ± 15.
Copper	208. ± 14.
Projectile Steel	156. ± 52.

In order to compare the results of the above analysis with previous work, the function

$$G\,(P/P_c) = e^{-P/P_c} \tag{27}$$

is substituted into equation (8) to obtain the relative force equation

$$F_r/F_c = \left(P/P_c\right) e^{-P/P_c} \tag{28}$$

Figure 6 shows the comparison of the function derived from the analysis with those functions in Figure 3. The exponential law shows excellent agreement with Amontons' and Archard's laws and passes through the range of values predicted from Bowden's theory. The data from the Franklin Institute covers the range of

$$.16 \leq P/P_c \leq 1.20 \tag{29}$$

That is to say, overtheir ranges of applicability, Amontons' and Archard's laws represent close approximations of the exponential equation (28).

B. Velocity Effects

In Palmer's overview paper "What About Friction,"[3] Ewald, Poschl and Prandtl's formula

$$\mu = \left[\frac{1 + 0.011\ V}{1 + 0.06\ V}\right] \mu_o \tag{30}$$

is cited as a possible relationship to express the correspondence of the coefficient of friction to sliding velocity where

μ_o is static coefficient of friction

V is the sliding velocity, in m/s.

Palmer further cites the work of Grosch and Plake in Germany in 1940. Their experiments used smooth bore cannon firings to measure the coefficient of friction versus velocity for steel on steel. The results of these experiments were summarized by the following formulation

$$\mu = 0.27 \left[\frac{1 + 0.0144\ V}{1 + .210\ V}\right] \tag{31}$$

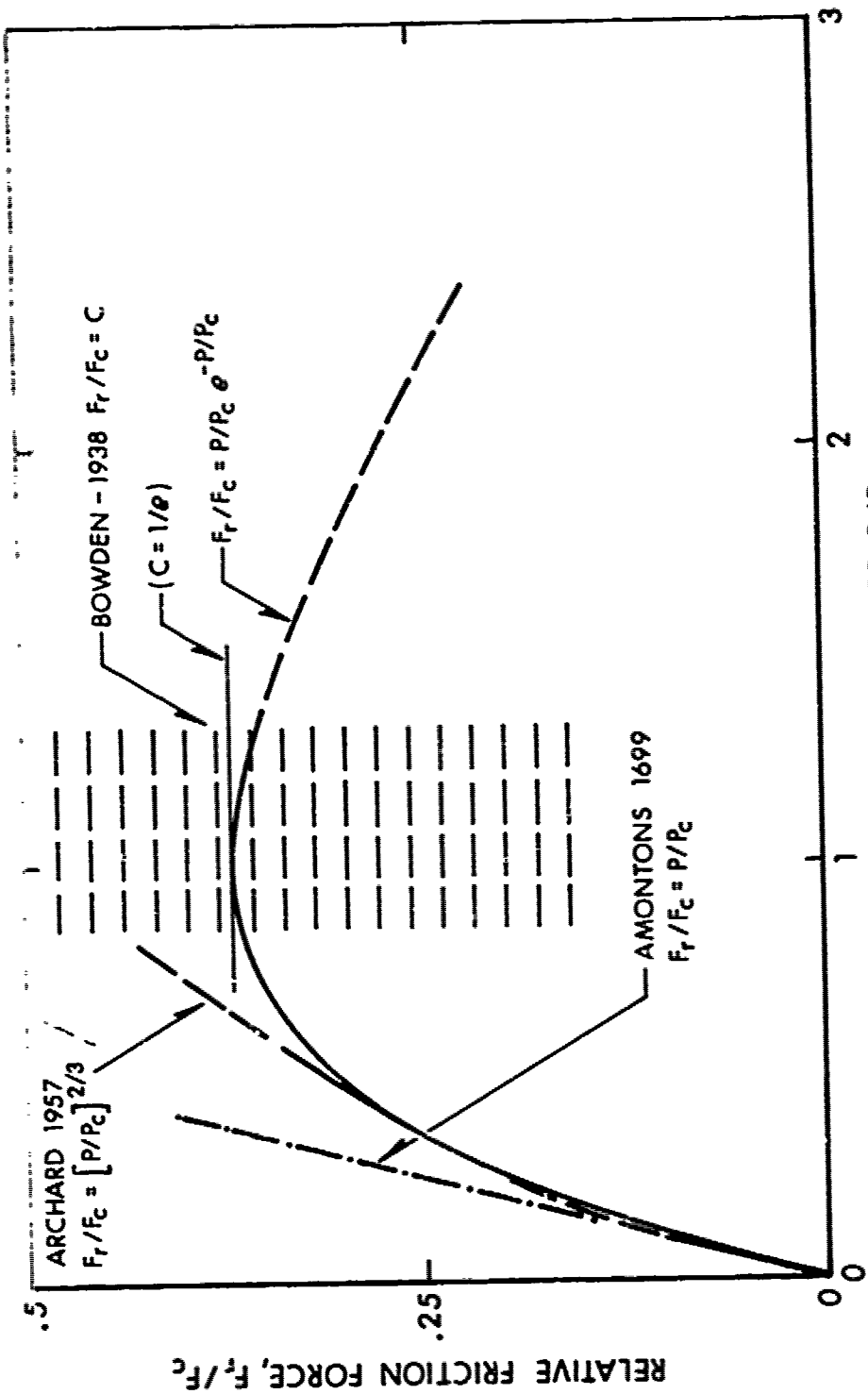

Figure 6. Plot Showing the Comparison of the Exponential Friction Law to the Laws Developed by Amontons, Bowdon and Archard.

In order to compare these formulations, they are nondimensionalized as follows. The basic form is restated as the relative coefficient of friction μ/μ_o ,a function of the relative velocity V/V_c.

$$\mu/\mu_o = \frac{1 + V/V_c}{1 + rV/V_c} \tag{32}$$

where $V_c = 1/a$; $r = b/a$

V_c is the critical velocity, an intrinsic property of the two materials

r is a dimensionless constant, an intrinsic property of the two materials

It should be stated that the two constants V_c and r are picked for convenience rather than from known specific properties. In this form, r becomes a characteristic of the equation to be evaluated in order to determine the relative differences between equations 30 and 31. For equation (30) r = 5.45 and for equation (31) r = 14.55. Figure 7 shows a comparison of the normalized form for the two formulations.

To evaluate the Franklin Institute data, sets of data were arranged according to material combinations to determine the correspondence of μ_i to V_i . Based on separability of variables, the data were assumed to follow

$$\mu_i = \mu_o f(V_i/V_c) e^{-P/P_c} \tag{33}$$

By defining

$$\mu_i^1 = \mu_i e^{P/P_c} \tag{34}$$

$$\mu_i^1 = \mu_o f(V_i/V_c) \tag{35}$$

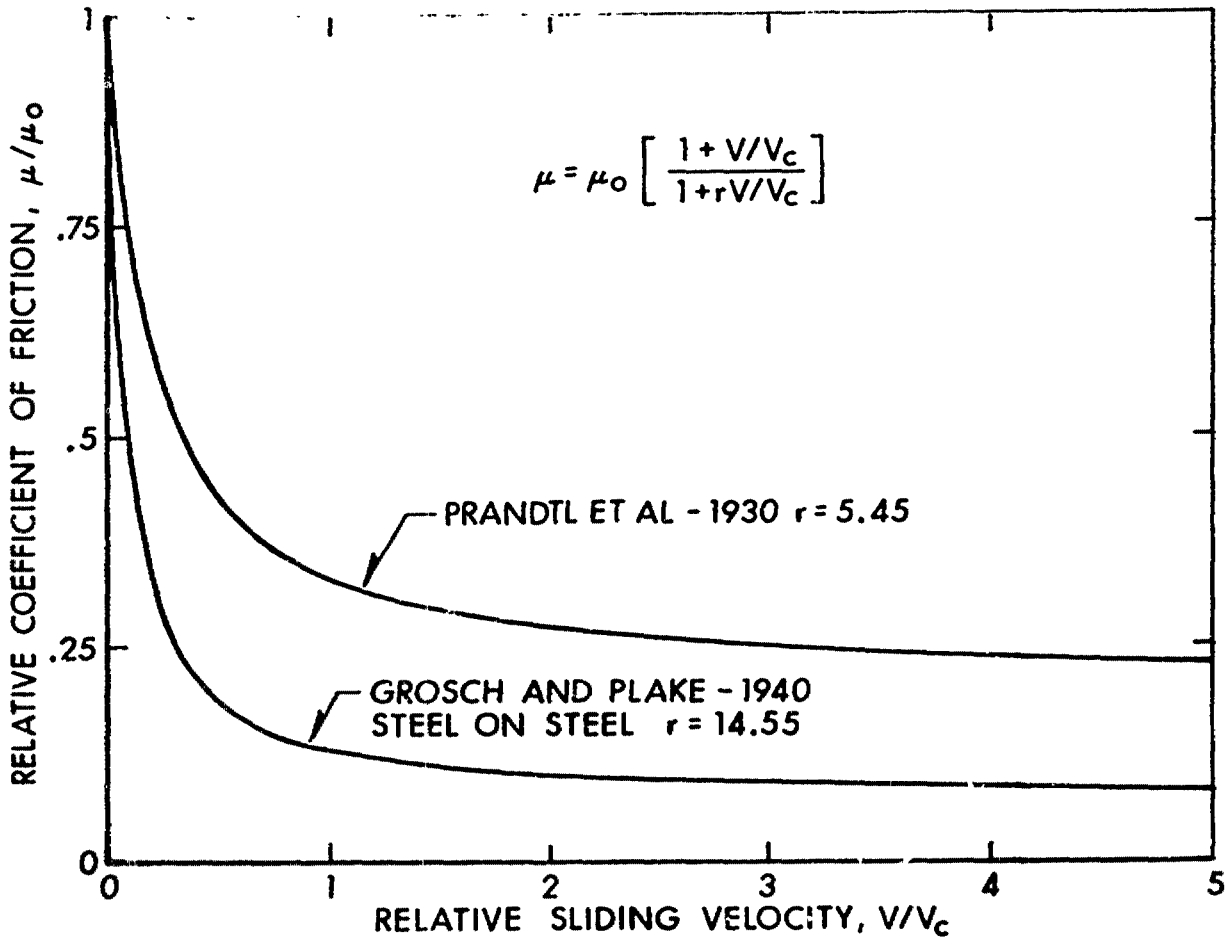

Figure 7. Plot Showing the Comparison of Prandtl's Equation to Grosch and Plake's Equation by Relating the Relative Coefficient of Friction Versus Relative Velocity.

μ_i was calculated for each data point in the appendices and arranged in a new table of μ_i versus V_i. Figure 8 shows a plot of μ_i versus V_i for gilding metal on steel. The points plotted show the mean value and the standard deviation. These sets of data were examined by use of the Theory of Least Squares to find the best fitting equation form as shown by equations (22a - 22e). The most accurate fitting form of all these forms was equation (22b) for all four materials; Table IV gives the calculated values of the constants for

$$\mu^1 = \mu_o \left[\frac{1 + aV}{1 + bV}\right] \tag{36}$$

and the constants for the nondimensionalized form

$$\mu^1 = \mu_o \left[\frac{1 + V/V_c}{1 + rV/V_c}\right] \tag{37}$$

Figure 9 shows the calculated mean curve and its standard deviation for gilding metal superimposed on the data shown in Figure 8.

TABLE IV. CALCULATED MEAN VALUES FOR b, a, μ_o V_c AND r FROM THE FRANKLIN INSTITUTE DATA

Material	μ_o	a,s/m	b,s/m	V_c,m/s	r
Gilding Metal	1.57 $\pm$ .15	.0019	.028	520	15.11
Annealed Iron	.66 $\pm$ .13	.0004	.0045	762	11.21
Copper	————	——	——	—	——*
Projectile Steel	————	——	——	—	——*

*Insufficient data exist to establish valid mean values.

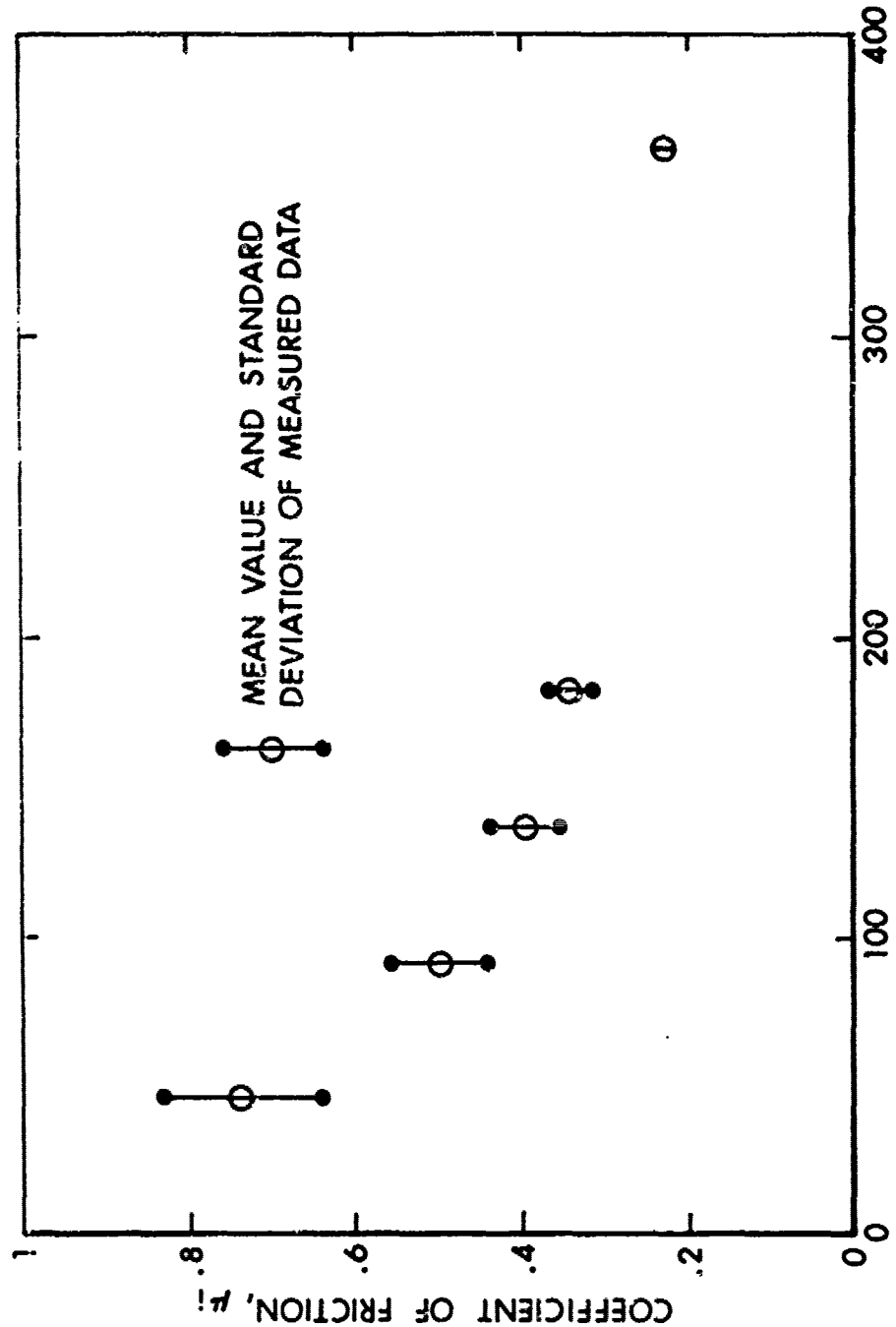

Figure 8. Plot Showing the Mean and Standard Deviation of the Pressure Corrected Coefficient μ_i Versus the Sliding Velocity V_i for Gliding Metal.

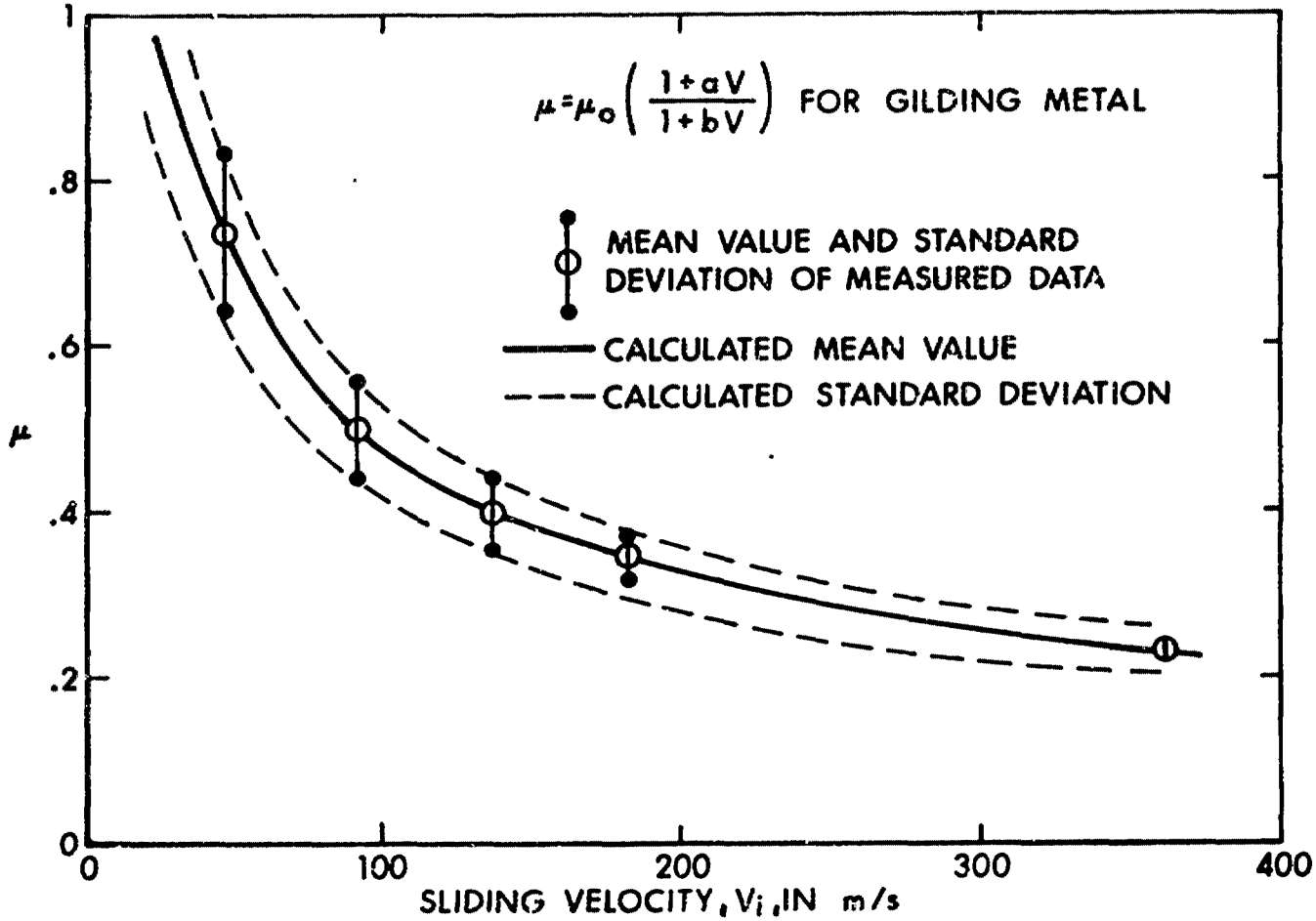

Figure 9. Plot of the Calculated and Measured Mean Standard Deviation of the Pressure Corrected Coefficient of Friction Versus Sliding Velocity for Gilding Metal.

The equation derived from the numerical analysis is identical in form to that proposed by Prandtl et al and that derived empirically by Grosch and Plake. Figure 10 shows a comparison of the resulting equation for the metals tested with the equations in Figure 7. The results for gilding metal and annealed iron have the greatest confidence level because of the number of data points available. The resulting values for the critical velocity and constant r for projectile steel and copper are considered to be inaccurate since they represent an extremely small sample size.

C. Heat Flux Effects

In order to evaluate the effect of heat flux, equations (33) and (37) are combined into the following expression

$$\mu = \mu_o e^{-P/P_c} \left[\frac{1 + V/V_c}{1 + rV/V_c} \right] \tag{38}$$

to calculate the coefficient of friction. From equations (38) and (2) the heat flux, Q is calculated by

$$Q = \mu_o e^{-P/P_c} \left[\frac{1 + V/V_c}{1 + rV/V_c} \right] PV \tag{39}$$

Using these parametric equations, the isobaric trajectories of the coefficient of friction versus the heat flux are calculated. Figure 11 shows the calculated isobaric trajectories for normal pressure of 20.69 MPa and 34.48 MPa for gilding metal sliding on steel superimposed on the corresponding data points for this pressure range. Figure 12 shows the calculated isobaric trajectories for the entire region defined by the data shown in Figure 2.

IV. EXTENSION OF THE RANGE OF VALIDITY OF THE PRESSURE FUNCTION FROM SHELL PUSHER EXPERIMENTS

The range of the pressure data from the Franklin Institute test does not go beyond

$$P/P_c \leq 1.2 \tag{40}$$

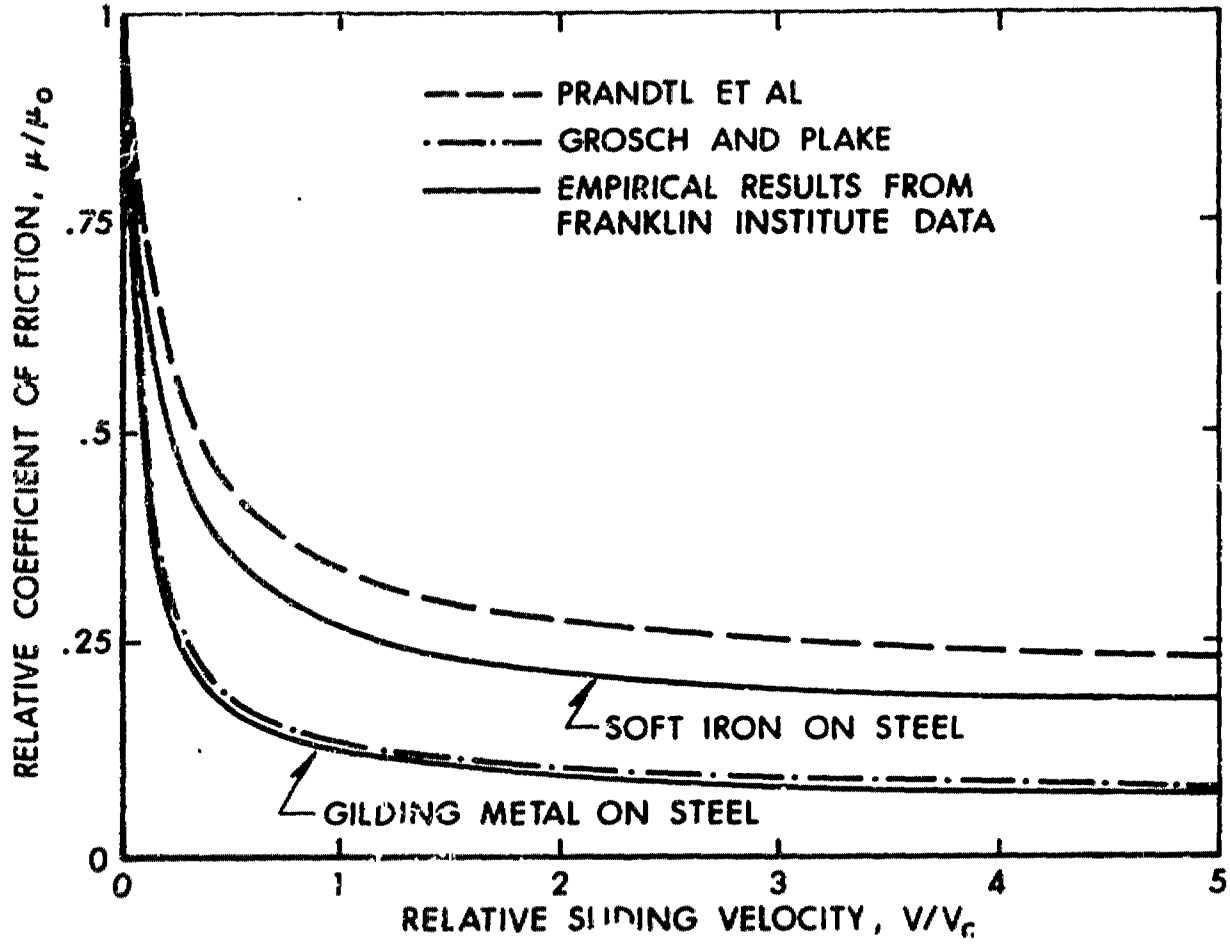

Figure 10. Plot Comparing Relative Coefficient of Friction Versus Relative Velocity from the Franklin Institute Data to the Results by Prandtl et al and Grosch and Plake.

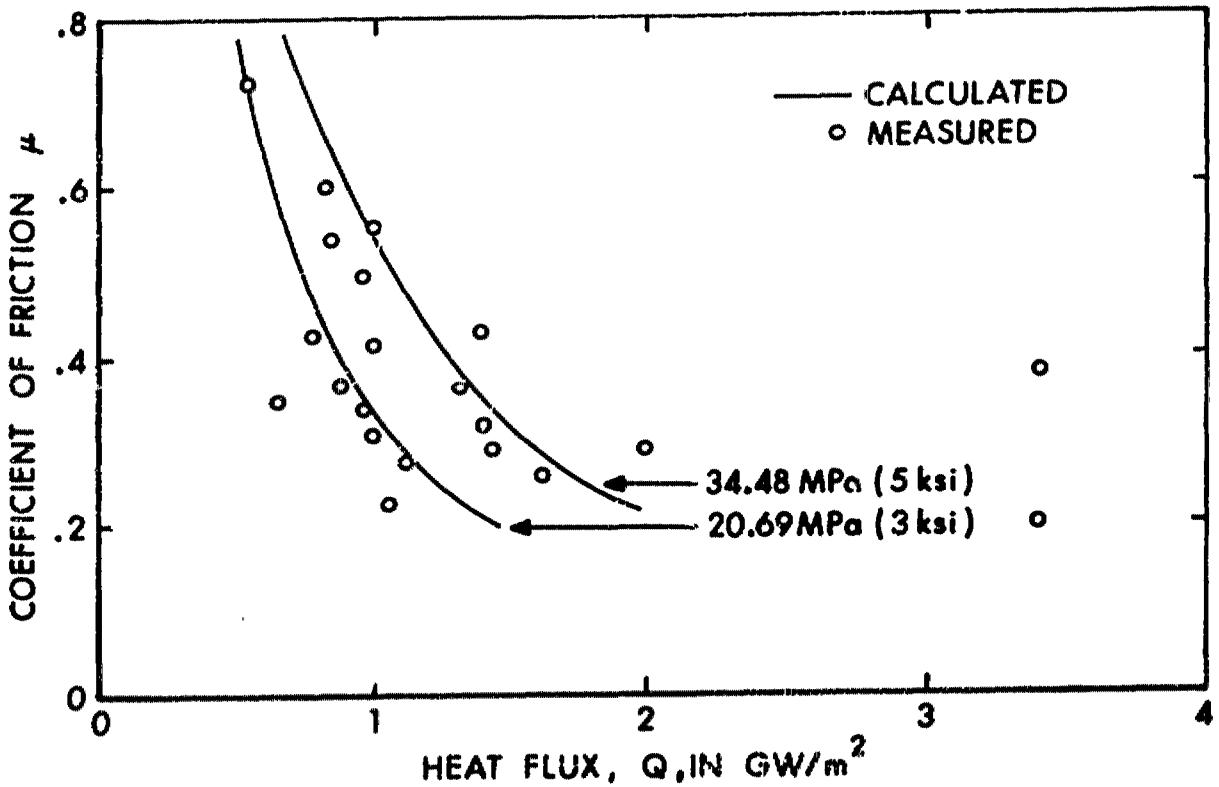

Figure 11. Plot Showing the Comparison of Measured Coefficient of Friction Versus Heat Flux for Pressure Between 20.69 MPa and 34.48 MPa to the Calculated 20.69 MPa and 34.48 Isobaric Trajectories for Gilding Metal.

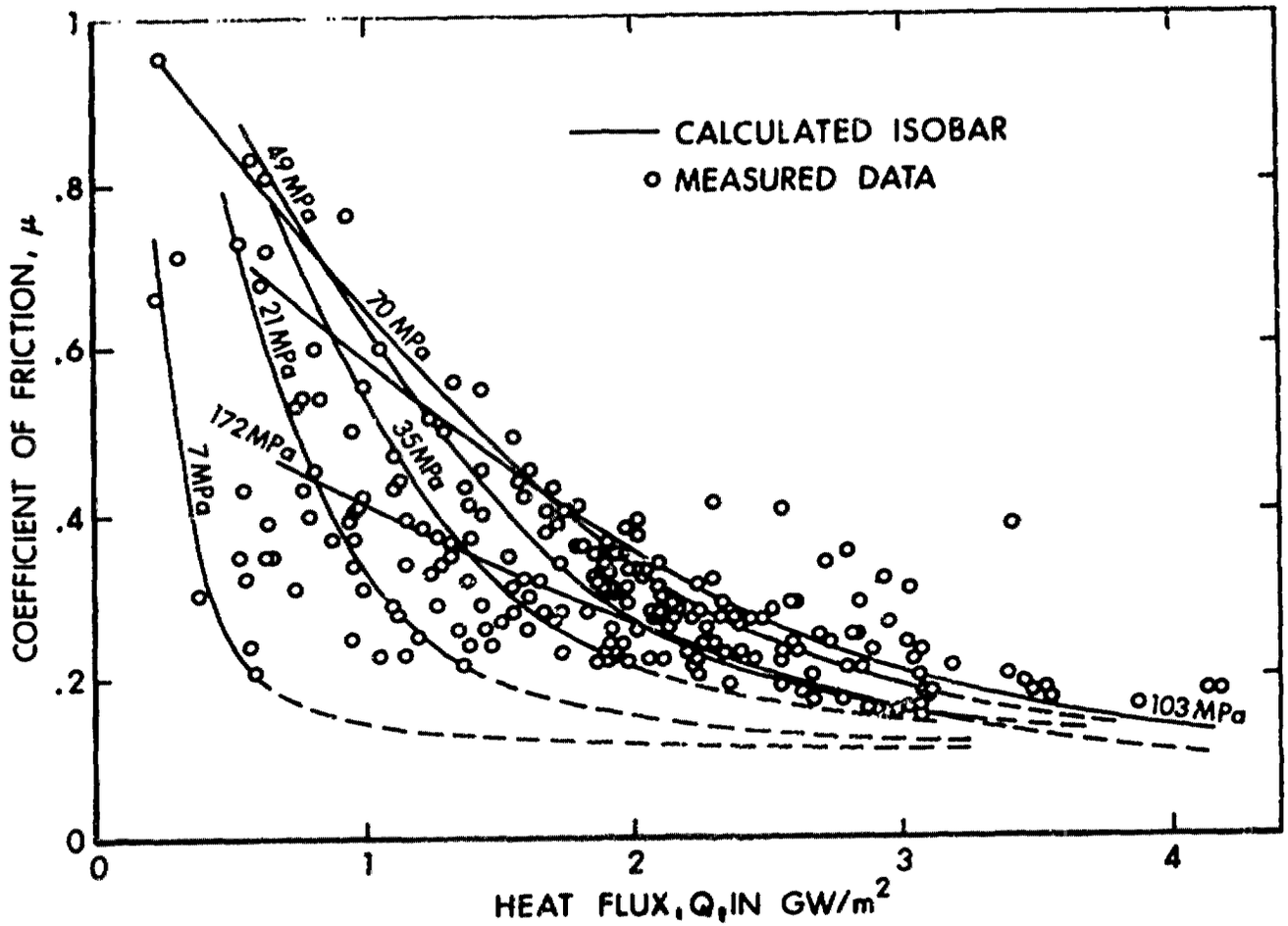

Figure 12. Plot Comparing the Calculated Isobaric Trajectories for Pressure Between 7 and 172 MPa to the Measured Data of the Coefficient of Friction Versus Heat Flux for Gilding Metal.

Thus, there is a question as to whether or not the derived empirical relationship from these data is valid for pressures experienced in the interior ballistic environment. To resolve this question, shell pusher experiments performed in the M483 Sticker Program were reviewed and analyzed.

These shell pusher tests were performed on an apparatus that mechanically pushes a projectile through a gun tube. The apparatus is shown in Figure 13 with an XM199 gun tube installed. During these tests, the force required to move the projectile and the strain at the tube surface induced by the rotating band pressure are measured. The band pressure is deduced from theory of elasticity calculations and the strain measurements. Appendix E gives the values of μ_o, μ, P_c, and P for these tests. The yield stress of the rotating band material was derived from hardness measurements made prior to each test on each projectile. M483 and M687 projectile bodies were used.

Because of the difference in the basic geometry (of the slider) between these tests and the pin-disc type of experiment, the shell pushing data were used to determine the behavior of the relative coefficient of friction, μ/μ_o, corresponding to the relative pressure, P/P_c. Calculating the relative coefficient of friction removes the geometry effects of the two experiments from the comparison of data. These data are compared with the calculated behavior from the empirical equation

$$\mu/\mu_o = e^{-P/P_c} \tag{41}$$

The sliding speed in these tests was held constant at 4×10^{-4} m/s. Figure 14 shows the results of these tests compared with the calculated relative friction. The relative pressure range of these data is

$$1.0 < P/P_c < 2.2 \tag{42}$$

These data are in excellent agreement with equation (41) and show that the equation is valid over the range

$$0 \leq P/P_c \leq 2.2 \tag{43}$$

which covers the range of relative pressures expected in the interior ballistic environments.

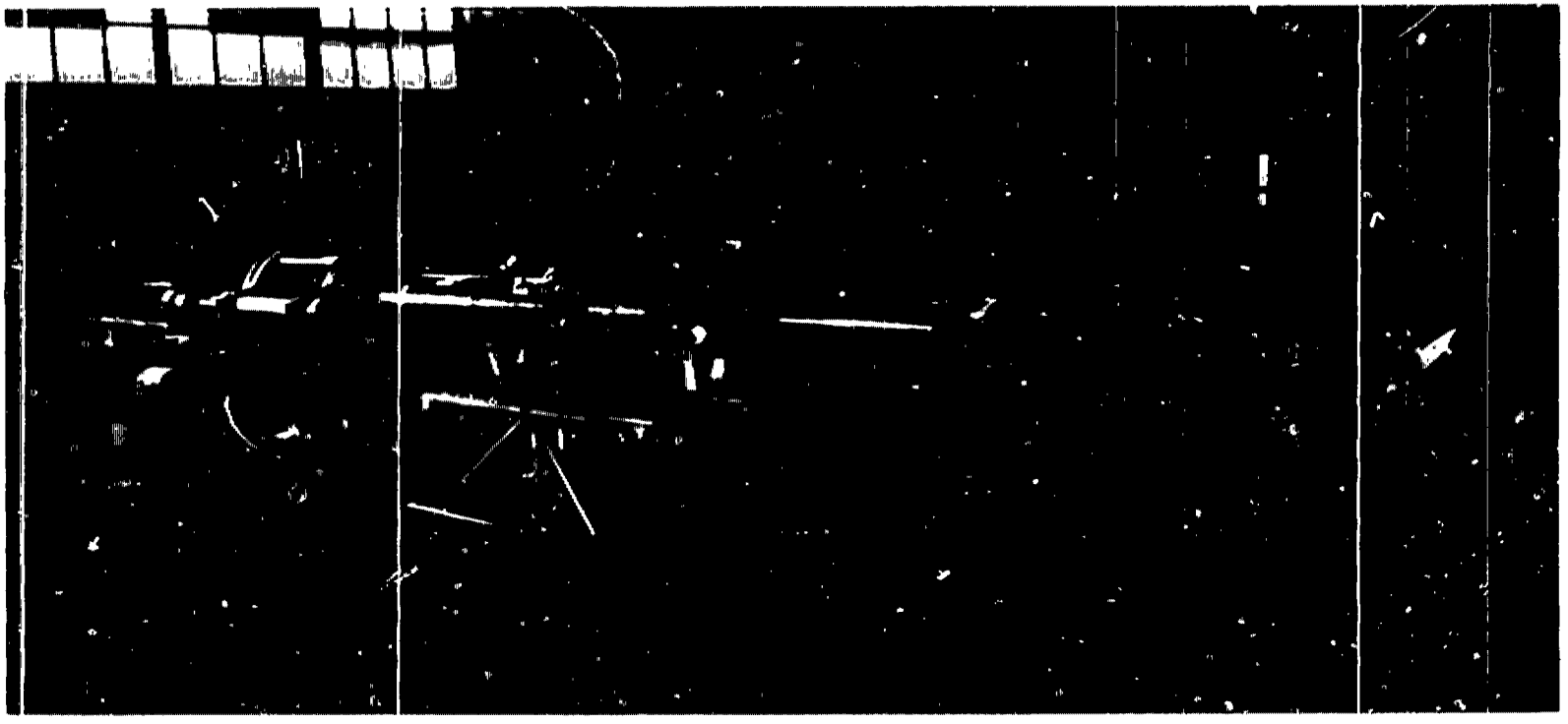

Figure 13. Photograph of the BRL Shell Pusher Apparatus with the XM199 Tube.

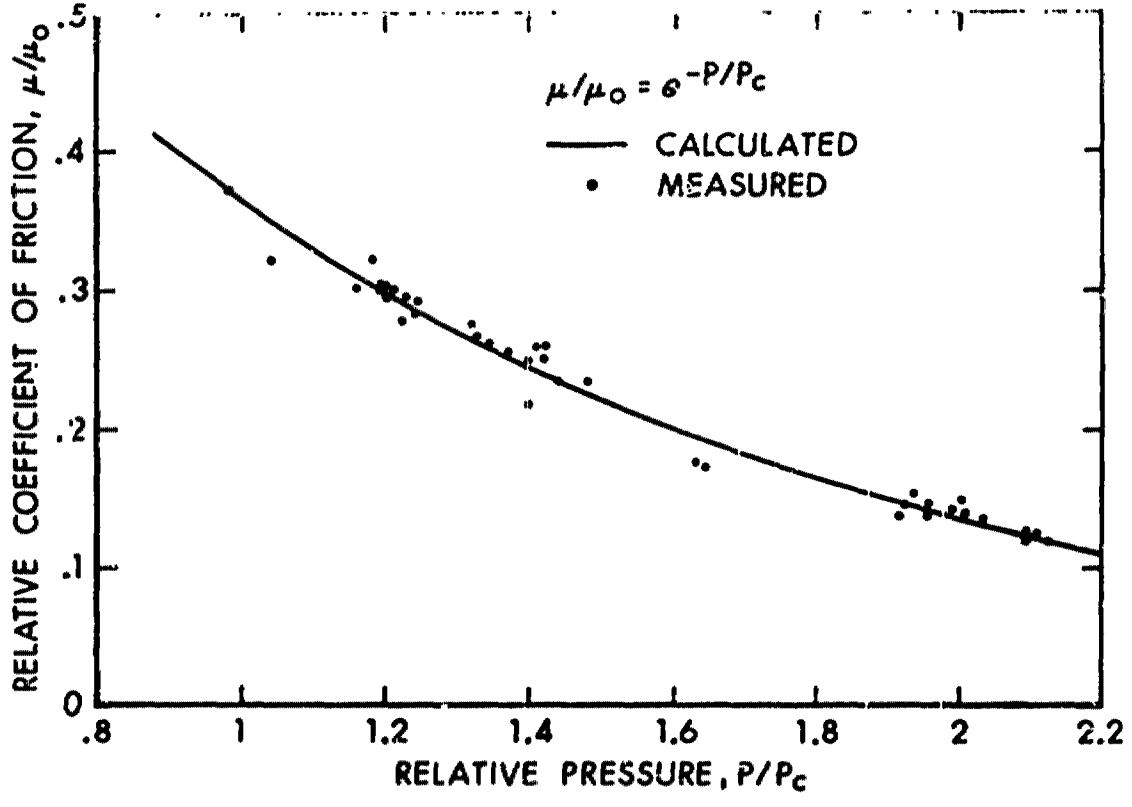

Figure 14. Plot Comparing the Exponential Friction Law to Measured Shell Pusher Data, Showing the Relative Coefficient of Friction Versus the Relative Pressure.

V. DIMENSIONAL ANALYSIS OF NUMERICAL RESULTS

The numerical results obtained only account for the effects of the bearing pressure, the sliding velocity and the static coefficient of friction. Since these data do not establish correlations of other parameters, such as geometry and thermodynamic properties of the slider, to the coefficient of friction, the results are examined by dimensional analysis techniques. These techniques, coupled with the observations from the numerical analyses and the results of other investigators, are used to determine the parameters for the following terms μ_o, P/P_c, V/V_c, and r. The resulting relationship then provides a more complete description of the process. However, the description is still an empirical one.

A. Observation From the Numerical Data

The numerical data indicate that P_c is in reality the yield strength of the slider

$$P_c = y \tag{44}$$

The numerical analysis shows that the constant r in the velocity portion of the empirical equation is dimensionless.

$$r = f(\pi_1 \cdots \pi_n) \tag{45}$$

where $\pi_1 \cdots \pi_n$ are dimensionless ratios of dimensioned quantities.

B. Observations from the Results of Other Investigators

Bowden's work which has been verified repeatedly by other experimenters defines

$$\mu_o = s/y \tag{46}$$

where s is the shear strength of the slider and y is the yield strength of the slider.

W. R. D. Wilson's analysis of lubrication by a melting solid slider[9] yields a nondimensional velocity term of

$$s = \frac{uV}{\ell\Lambda} \tag{47}$$

where u is the viscosity of the molten slider material; ℓ is the characteristic length of the slider parallel to the velocity vector; Λ is the

[9] *W. R. D. Wilson, "Lubrication by a Melting Solid," Journal of Lubrication Technology, Transactions of the ASME, Paper No. 75, Lub-26, 7 Jul 75.*

volumetric latent heat of melting of the slider material. Wilson's analysis is based on the assumption that the heat generated by viscous shearing in the film provides the latent heat necessary to melt the adjacent surface (in this case, the slider). Since this assumption and the experiment were for ice surfaces, the ambient temperature was approximately the melting temperature of the slider. Therefore, one would expect the constant Λ occurring in the equation to be replaced by the total volumetric heat capacity

$$C_v \Delta T + \Lambda = K \tag{48}$$

where; C_v is the volumetric heat capacity of the slider material, in J/m^3K; ΔT is the difference between the melting temperature and the ambient temperature, in K; Λ is the volumetric heat of melting, in J/m^3. From thermodynamic considerations, specific properties should be used in the problem. Hence, one can assume that the parameter of kinematic viscosity is more appropriate than viscosity. In both cases, the slider length in the direction of the velocity vector can be assumed to be a key parameter.

C. Dimensional Analyses

Taking the parameters discussed above and casting them in implicit form

$$f(s, y, P, V, C_v, \Lambda, \Delta T, v, \ell) = 0 \tag{49}$$

where s = the shear strength of the slider material, in Pa.
y = the yield strength of the slider material, in Pa.
P = the normal pressure, in Pa.
V = the sliding velocity, in m/s.
C_v = the volumetric heat capacity of the slider material, in J/m^3K.
Λ = the heat of fusion of the slider material, in J/m^3.
ΔT = the temperature of fusion minus the ambient temperature, in K°.
v = the kinematic viscosity, in m^2/s.
ℓ = the length of the slider parallel to the velocity vector, in m.

The following nondimensional terms are derived by the Buckingham Pi Theorem.

a) $\pi_1 = s/y$

b) $\pi_2 = P/y$

c) $\pi_3 = \frac{\ell V}{v}$

d) $\pi_4 = \frac{C_v \Delta T}{y}$

e) $\pi_5 = \frac{\Lambda}{y}$ (50)

From the dimensional analysis and the numerical analysis, we have the following substitution:

a) $\mu_o = s/y$

b) $P/P_c = P/y$

c) $V/V_c = \frac{c\ell V}{v}$

d) $r = f\left(\frac{C_v \Delta T + \Lambda}{y}\right)$ (51)

where c is an arbitrary constant and f denotes an undefined function.

Substituting these quantities into equation (38), the following equation is derived

$$\mu = s/y \left[\frac{1 + c\frac{\ell V}{v}}{1 + f\left(\frac{C_v \Delta T + \Lambda}{y}\right)\frac{c\ell V}{v}}\right] e^{-P/y} \quad (52)$$

VI. SUMMARY OF RESULTS

Through the numerical analyses of the Franklin Institute experimental data for dry sliding friction at high pressures and velocities, an empirical equation relating the dynamic coefficient of friction to the static coefficient of friction, normal pressure and sliding speed has been developed for an elastic-plastic slider sliding on a rigid surface. The equation derived from the numerical analysis contains four critical constants: static coefficient of friction, critical pressure, critical velocity and r, a dimensionless ratio. By examining classical and modern friction theory and application of dimensional analysis techniques, these critical constants have been resolved into material, geometric and thermodynamic parameters as shown in equation (52).

A. Behavior Due to Normal Pressure

The relationship of the coefficient of friction to normal pressure is an exponential law which agrees closely with the classical law and Archard's power law in their respective regions of validity. In addition, the friction force generated by the exponential law behaves in a monotonically increasing manner with increasing pressure through the elastic regime and in a monotonically decreasing manner with increasing pressure beyond the point of incipient plastic flow. The maximum force occurs at the yield strength of the material and the ratio of the actual friction force to classical friction force is 1/e. The behavior, in general, represents a transition from one friction law to another and is valid to pressures in excess of twice the yield strength.

B. Behavior Due to Sliding Velocity

The relationship of the coefficient of friction to velocity is identical in form to the equation proposed by Prandtl et al, and to the empirical equation developed by Grosch and Plake. In addition, this equation shows the same character as the data presented by Bowden and Brunton.[10] These investigators' experiments extend to velocities of 1000 m/s, showing that the equation is usable for the majority of interior ballistic problems and that the probability of its validity for higher velocities is quite high. The velocity term in the equation is the Reynolds number, which allows the establishment of laws for scaling from experimental geometry to rotating band geometry. The dimensionless constant r in the velocity term is a function of the thermodynamic and yield strength properties of the material. However, this function has not been completely determined and will require additional data from highly specific experiments to establish the proper functional relationships.

C. A Caveat

The empirical equations generated from the Franklin Institute experimental data and the BRL Shell Pusher Data apply to cases where an elastic-plastic slider is sliding without lubricant on a surface which has appreciably higher strengths than the slider. The equations developed cannot be construed to be valid for visco-elastic sliders or for soft glide surfaces.

Recent measurements by R. S. Montgomery[11] (not yet published) indicate that soft iron undergoes a phase transition during the sliding process that changes the response of the slider to velocity. The above equations do not account for phase changes in the material.

VII. RECOMMENDATIONS

There is no doubt in the authors' minds that a valid empirical relationship for dynamic friction versus normal pressure has been established. However, the velocity relationship remains incomplete.

A. Dimensional Effects

A series of experiments where changes in the geometry are made are required in order to verify the geometric dependency of the coefficient of friction

$$V/V_c = c \frac{\ell V}{v} \qquad (53)$$

---

[10] *F. Bowden and J. Brunton, "The Behavior of Materials in a High Speed Environment," Proceedings of the Third Symposium on Naval Structural Mechanics held in New York, January 1963, Pergamon Press, New York, 1963.*

[11] *R. S. Montgomery, Watervliet Arsenal, NY. Phone conversation on 4 June 1976.*

B. Thermodynamic Effects

Two series of experiments are recommended:

(1) A series of experiments where the surface temperature of the slider is varied to determine the relationship

$$r = f\left(\frac{C_v \Delta T + \Lambda}{y}\right) \tag{54}$$

(2) A series of experiments where the yield strength of the material is varied to determine the relationship shown for r in equation (54).

C. Interior Ballistic Modeling

The velocity relationship coupled with static resistance profiles from projectile push test should be used in place of the traditional lumped profile system as a first-order approximation of the bore resistance in interior ballistic codes. Such a model can be used to determine the initial motion of the projectile and its tendencies to stick.

ACKNOWLEDGEMENTS

The authors greatly appreciate the enthusiastic support they received from Mr. A. S. Elder and Dr. R. Loder of BRL and Dr. R. S. Montgomery of Watervliet Arsenal.

REFERENCES

1. R. S. Montgomery, "Friction and Wear at High Sliding Speeds," Wear, Vol 36 (1976), pp 275-298.

2. W. E. Baker, P. S. Westine and F. T. Dodge, Similarity Methods in Engineering Dynamics, Hayden Book Company, Inc, Rochelle Park, NJ, 1973, Chapter 3.

3. F. Palmer, "What About Friction," American Journal of Physics, 1949.

4. F. P. Bowden and D. Tabor, Friction and Lubrication, John Wiley and Sons, Inc, New York, 1956.

5. J. F. Archard, "Single Contacts and Multiple Encounters," Journal of Applied Physics, 1961, Vol 32.

6. A. Gemant, Frictional Phenomena, Chemical Publishing Company, Inc, Brooklyn, NJ, 1950.

7. A. M. Freudenthal, The Inelastic Behavior of Engineering Materials and Solid Structures, John Wiley and Sons, New York, 1950, Page 261.

8. R. W. Hamming, Numerical Methods for Scientists and Engineers, McGraw-Hill, New York, 1962, pp 223-225.

9. W. R. D. Wilson, "Lubrication by a Melting Solid," Journal of Lubrication Technology, Transactions of the ASME, Paper No. 75, Lub-26, 7 Jul 75.

10. F. Bowden and J. Brunton, "The Behavior of Materials in a High Speed Environment," Proceedings of the Third Symposium on Naval Structural Mechanics held in New York, January 1963, Pergamon Press, New York, 1963.

11. R. S. Montgomery, Watervliet Arsenal, NY. Phone conversation on 4 June 1976.

APPENDIX A

Specimen Composition and Friction Data* for Gilding Metal

*Extracted from R. S. Montgomery, "Friction and Wear at High Sliding Speeds," Benet Laboratory Report No. WVT-TR-75028, June 1975.

Table AI

Composition of Gilding Metal

Lot	Cu%	Pb%	Zn%	Fe%	Remainder %
1	89.93	.01	9.94	.02	.10
2	90.25	.02	9.65	.03	.05

TABLE AII

Friction Data for Gilding Metal

Velocity m/s	Pressure MPa	Coefficient of Friction
45.7	18.62	0.81
	20.00	0.72
	20.69	0.38
	20.69	0.00
	26.90	0.00
	28.28	0.76
	31.03	0.60
	33.10	0.00
	35.86	0.54
	44.14	0.00
	44.83	0.00
	53.10	0.56
	56.55	0.52
	60.69	0.55
	82.07	0.44
	82.76	0.00
	87.59	0.00
	94.48	0.40
	112.41	0.00
	118.62	0.37
	126.90	0.00
	135.17	0.32
91.4	5.24	0.71
	10.34	0.68
	12.41	0.34
	15.17	0.00
	15.17	0.30
	15.17	0.42
	15.17	0.43
	15.86	0.53
	16.55	0.00
	17.93	0.00
	17.93	0.35
	20.00	0.32
	20.69	0.35
	20.69	0.35
	20.69	0.43
	20.69	0.55
	22.07	0.50

TABLE AIII

Friction Data for Gilding Metal

Velocity m/s	Pressure MPa	Coefficient of Friction
91.4	22.76	0.00
	26.90	0.41
	27.59	0.42
	27.59	0.47
	28.28	0.39
	29.66	0.37
	29.66	0.44
	29.66	0.50
	32.41	0.34
	35.86	0.38
	35.86	0.43
	36.55	0.00
	37.93	0.00
	37.93	0.45
	37.93	0.49
	39.31	0.41
	40.69	0.40
	41.38	0.00
	41.38	0.00
	42.07	0.45
	42.76	0.33
	43.45	0.42
	44.14	0.29
	44.14	0.34
	44.14	0.34
	44.14	0.37
	45.52	0.43
	47.59	0.00
	49.66	0.37
	50.34	0.38
	50.34	0.39
	51.72	0.29
	51.72	0.35
	51.72	0.39
	51.72	0.41
	57.93	0.36
	58.62	0.37
	59.31	0.00
	60.69	0.32
	60.69	0.34

TABLE AIV

Friction Data for Gilding Metal

Velocity m/s	Pressure MPa	Coefficient of Friction
91.4	60.69	0.38
	60.69	0.39
	62.07	0.35
	62.76	0.35
	63.45	0.00
	64.14	0.34
	64.83	0.28
	65.52	0.41
	66.21	0.00
	67.59	0.00
	67.59	0.32
	69.66	0.31
	70.34	0.28
	70.34	0.31
	70.34	0.34
	71.03	0.33
	72.41	0.30
	73.10	0.40
	73.79	0.27
	74.48	0.32
	77.93	0.31
	78.62	0.29
	79.31	0.32
	80.69	0.00
	81.79	0.30
	82.76	0.32
	84.14	0.28
	84.14	0.28
	84.83	0.00
	86.21	0.27
	88.97	0.27
	89.66	0.27
	90.34	0.26
	91.03	0.35
	92.41	0.27
	92.41	0.29
	93.10	0.24
	99.31	0.00
	101.38	0.26
	104.14	0.24

TABLE AV

Friction Data for Gilding Metal

Velocity m/s	Pressure MPa	Coefficient of Friction
91.4	104.14	0.28
	105.52	0.32
	106.21	0.26
	112.41	0.31
	120.69	0.25
	125.52	0.00
	126.21	0.27
	127.59	0.00
	128.28	0.22
	131.03	0.25
	132.41	0.00
	137.24	0.00
	156.55	0.00
121.9	16.55	0.00
	24.14	0.00
	28.97	0.00
	33.10	0.00
	35.86	0.00
	41.38	0.00
	47.59	0.00
	52.41	0.00
	55.17	0.00
	61.38	0.00
	62.76	0.00
	64.14	0.00
	75.86	0.00
	84.14	0.00
	93.79	0.00
	100.69	0.00
	104.14	0.00
	110.34	0.00
	123.45	0.00
	137.24	0.00
	148.28	0.00
137.2	11.03	0.54
	12.41	0.39
	15.17	0.40
	17.93	0.24

TABLE AVI

Friction Data for Gilding Metal

Velocity m/s	Pressure MPa	Coefficient of Friction
137.2	17.93	0.37
	18.62	0.40
	19.31	0.43
	23.45	0.39
	26.21	0.34
	28.97	0.35
	29.66	0.25
	30.34	0.39
	33.79	0.32
	35.17	0.23
	37.93	0.31
	37.93	0.36
	38.62	0.23
	38.62	0.29
	40.69	0.30
	42.07	0.37
	44.14	0.33
	44.83	0.33
	46.21	0.28
	46.90	0.24
	46.90	0.31
	49.66	0.30
	49.66	0.31
	50.34	0.28
	54.48	0.31
	56.55	0.29
	57.93	0.23
	59.31	0.28
	62.07	0.28
	63.45	0.24
	63.45	0.26
	64.83	0.23
	66.21	0.27
	66.90	0.27
	68.28	0.28
	68.28	0.29
	69.66	0.27
	69.66	0.29
	70.34	0.27
	71.72	0.24

TABLE AVII

Friction Data for Gilding Metal

Velocity m/s	Pressure MPa	Coefficient of Friction
137.2	72.41	0.22
	73.10	0.23
	74.48	0.29
	78.62	0.22
	78.62	0.23
	79.31	0.23
	80.69	0.22
	86.90	0.23
	92.41	0.23
	95.17	0.19
	95.86	0.24
	97.24	0.23
	102.07	0.19
	102.76	0.21
	108.28	0.20
	116.55	0.21
	117.93	0.20
	132.41	0.18
179.8	24.14	0.00
	47.59	0.00
	73.79	0.00
	95.17	0.00
	117.24	0.00
182.9	13.79	0.31
	15.86	0.00
	17.93	0.00
	17.93	0.31
	19.31	0.37
	21.38	0.00
	23.45	0.28
	28.28	0.32
	29.66	0.26
	32.41	0.26
	32.41	0.27
	33.10	0.32
	33.79	0.24
	34.48	0.33
	35.17	0.26

TABLE AVIII

Friction Data for Gilding Metal

Velocity m/s	Pressure MPa	Coefficient of Friction
182.9	35.86	0.00
	42.76	0.26
	43.45	0.28
	45.52	0.34
	46.90	0.27
	49.66	0.22
	49.66	0.22
	49.66	0.22
	51.72	0.22
	55.17	0.22
	55.17	0.24
	57.93	0.00
	60.00	0.24
	60.69	0.21
	62.07	0.24
	62.07	0.25
	64.14	0.23
	64.83	0.20
	65.52	0.24
	65.52	0.25
	66.90	0.22
	74.48	0.00
	76.55	0.20
	77.24	0.23
	77.93	0.00
	77.93	0.22
	78.62	0.21
	79.31	0.00
	90.34	0.17
	92.41	0.00
	97.24	0.20
	98.62	0.18
	103.45	0.16
	104.83	0.19
	108.97	0.16
	111.03	0.18
	112.41	0.18
	120.69	0.17
	126.90	0.00
	131.72	0.18

TABLE AIX

Friction Data for Gilding Metal

Velocity m/s	Pressure MPa	Coefficient of Friction
182.9	133.10	0.00
	133.79	0.18
	140.69	0.00
	181.38	0.00
365.8	46.90	0.17
	49.66	0.18
	52.41	0.16
	55.17	0.16
	69.66	0.15
	69.66	0.16

APPENDIX B

Specimen Composition and Friction Data* for Annealed Iron

*Extracted from R. S. Montgomery, "Friction and Wear at High Sliding Speeds," Benet Laboratory Report No. WVT-TR-75028, June 1975

TABLE BI

Composition of Annealed Iron

Lot	Fe%	C%	Mn%	P%	S%	Si%
1	99.922	.017	.020	.008	.023	.010
2	99.934	.023	.018	.007	.017	.001

TABLE BII

Friction Data for Soft Iron

Velocity m/s	Pressure MPa	Coefficient of Friction
45.7	42.76	0.42
	51.03	0.43
	56.55	0.34
	66.90	0.30
	68.28	0.44
	100.69	0.33
	124.14	0.31
91.4	4.14	1.13
	9.66	0.33
	12.41	0.58
	13.79	0.51
	20.69	0.31
	20.69	0.42
	22.76	0.46
	27.59	0.36
	27.59	0.42
	31.03	0.42
	33.10	0.27
	35.86	0.39
	37.93	0.27
	40.69	0.34
	44.83	0.26
	44.83	0.38
	53.79	0.24
	54.48	0.32
	57.24	0.35
	60.00	0.29
	60.00	0.34
	65.52	0.32
	66.90	0.30
	66.90	0.34
	67.59	0.23
	68.28	0.31
	68.97	0.26
	71.72	0.31
	75.17	0.24
	78.62	0.32
	81.38	0.29
	84.14	0.26

TABLE BIII

Friction Data for Soft Iron

Velocity m/s	Pressure MPa	Coefficient of Friction
91.4	88.97	0.24
	95.86	0.29
	98.62	0.31
	102.07	0.28
	106.90	0.24
	106.90	0.27
	115.17	0.28
	128.28	0.26
	129.66	0.27
	134.48	0.28
	135.17	0.27
	138.62	0.21
	140.00	0.27
137.2	6.21	0.40
	12.41	0.33
	15.86	0.35
	22.07	0.28
	27.59	0.33
	31.03	0.27
	40.00	0.26
	40.00	0.32
	41.38	0.22
	42.07	0.31
	44.83	0.24
	51.03	0.29
	52.41	0.23
	63.45	0.27
	68.97	0.28
	69.66	0.21
	71.03	0.26
	74.48	0.21
	78.62	0.21
	79.31	0.24
	81.38	0.20
	89.66	0.20
	90.34	0.23
	99.31	0.25
	103.45	0.20
	131.72	0.21

TABLE BIV

Friction Data for Soft Iron

Velocity m/s	Pressure MPa	Coefficient of Friction
137.2	144.14	0.15
182.9	6.90	0.42
	15.17	0.27
	15.17	0.36
	22.75	0.25
	25.52	0.26
	27.59	0.25
	31.03	0.25
	34.48	0.25
	35.86	0.25
	41.38	0.25
	44.14	0.25
	48.97	0.25
	49.66	0.24
	55.86	0.25
	57.24	0.20
	66.90	0.23
	68.28	0.23
	74.48	0.22
	75.17	0.19
	82.07	0.20
	86.90	0.17
	92.41	0.20
	92.41	0.21
	93.10	0.16
	98.62	0.16
	98.62	0.20
	105.52	0.17
	106.21	0.18
	109.66	0.18
	111.72	0.18
	117.93	0.15
	123.45	0.18
	129.66	0.17
	137.24	0.16
274.3	27.59	0.24
	43.45	0.20
	69.66	0.16

TABLE BV

Friction Data for Soft Iron

Velocity m/s	Pressure MPa	Coefficient of Friction
274.3	78.62	0.15
	89.66	0.15
	100.00	0.17
	111.03	0.17

APPENDIX C

Specimen Composition and Friction Data* for Copper

*Extracted from R. S. Montgomery, "Friction and Wear at High Sliding Speeds," Benet Laboratory Report No. WVT-TR-75028, June 1975

TABLE CI

Composition of Copper

Lot	Cu%	Fe%	Zn%	Al%	Ni%	Pb%
1	99.88	0.012	.005	.004	.001	.003
2	99.96	.006	Nil	.002	.0005	.005

Lot	Pb%	Mn%	Sn%	Mg%	Ag%	Cd%
1	.003	Nil	.004	.004	.002	Nil
2	.005	Nil	.002	.004	.008	Nil

Lot	Si%	Cr%	Mo%	V%
1	.09	Nil	Nil	Nil
2	.03	Nil	Nil	Nil

TABLE CII

Friction Data for Copper

Velocity m/s	Pressure MPa	Coefficient of Friction
45.7	17.93	0.00
	22.76	1.06
	25.52	1.13
	26.21	1.10
	26.21	1.13
	27.59	0.00
	27.59	0.00
	28.28	1.07
	29.66	1.02
	31.72	0.59
	40.00	0.86
	41.38	0.00
	41.38	0.00
	41.38	0.77
	41.38	0.82
	41.38	0.75
	41.38	0.77
	41.38	0.85
	41.38	1.07
	41.38	1.33
	42.76	0.73
	45.52	0.61
	49.66	0.47
	52.41	0.63
	52.41	0.68
	56.55	0.79
	57.24	0.60
	73.79	0.59
	76.55	0.61
	82.07	0.87
	87.59	0.66
	88.97	0.66
	90.34	0.60
	91.72	0.59
	94.48	0.59
	94.48	0.59
	94.48	0.60
182.9	24.83	0.38
	37.24	0.35

TABLE CIII

Friction Data for Copper

Velocity m/s	Pressure MPa	Coefficient of Friction
182.9	45.52	0.27
	45.52	0.31
	73.79	0.26
	75.86	0.25
	76.55	0.27
	76.55	0.28
	82.07	0.30
	82.07	0.27
	87.59	0.15
	112.41	0.23
	146.90	0.21
	157.93	0.17
	159.31	0.18
	162.07	0.17
	170.34	0.16
	180.69	0.15
274.3	28.28	0.21
	28.97	0.24
	33.10	0.27
	90.34	0.24
	93.10	0.25
	93.10	0.25
	95.86	0.24
	115.17	0.18
	115.17	0.19
	116.55	0.19
	117.93	0.17
	117.93	0.18
	122.07	0.18
365.8	31.72	0.30
	39.31	0.26
	41.38	0.20
	41.38	0.23
	77.93	0.19
	79.31	0.17
	83.45	0.22
	87.59	0.24
	123.45	0.18

TABLE CIV

Friction Data for Copper

Velocity m/s	Pressure MPa	Coefficient of Friction
365.8	149.66	0.13
	159.31	0.13
457.2	38.62	0.26
	41.38	0.18
	81.38	0.19
	84.83	0.19
	128.97	0.15
548.6	40.00	0.22
	41.38	0.26
	82.76	0.18
	126.90	0.15

APPENDIX D

Specimen Composition and Friction Data* for Projectile Steel

*Extracted from R. S. Montgomery, "Friction and Wear at High Sliding Speeds," Benet Laboratory Report No. WVT-TR-75028, June 1975

TABLE DI

Composition of Projectile Steel

Fe%	C%	Mn%	P%	S%	Si%
98.243	0.529	0.93	.034	.010	.254

TABLE DII

Friction Data for Projectile Steel

Velocity m/s	Pressure MPa	Coefficient of Friction
182.9	24.14	0.29
	24.83	0.28
	39.31	0.24
	76.55	0.26
	81.38	0.24
	82.07	0.23
	82.07	0.23
	82.07	0.27
	82.76	0.28
	83.45	0.30
	85.52	0.27
	88.97	0.28
274.3	57.24	0.30
	73.79	0.35
	76.55	0.24
	79.31	0.22
	79.31	0.24
	79.31	0.24
	82.07	0.00
	82.07	0.00
365.8	37.24	0.37
	72.41	0.30
	73.79	0.30
	75.17	0.25
	75.17	0.29
	76.55	0.27
	78.62	0.30
	124.83	0.21
	125.52	0.24
	128.97	0.23
	133.79	0.24
	135.86	0.22
	162.07	0.22

APPENDIX E

Friction Data from BRL Shell Pusher Tests of the XM687 and M483 155mm Projectiles in the XM199 and M185 155mm Gun Tubes

TABLE EI

Shell Pusher Data for Friction and Pressure
on XM199 155mm Tube

Run #	Projectile	P, in MPa	μ	μ_o	P_c, in MPa
1	XM687	217	.206	.730	172
		229	.193		
		243	.182		
		232	.191		
2	M483	179	.226	.707	172
		229	.196		
		243	.183		
		236	.177		
		211	.209		
		211	.209		
		207	.212		
		200	.220		
3	XM687	200	.225	.750	172
		243	.186		
		257	.176		
		247	.173		
4	M483	168	.292	.783	172
		204	.257		
		207	.240		
		211	.229		
		207	.230		
		207	.230		
		208	.228		
		214	.222		

TABLE EII

Shell Pusher Data for Friction and Pressure
on M185 155mm Tube

Run #	Projectile	P, in MPa	μ	μ_o	P_c, in MPa
5	XM687	311	.248	1.2	172
		345	.174		
		336	.165		
		332	.167		
		[illegible]	.179		
		332	.179		
		336	.176		
		282	.211		
6	M483	282	.273	1.535	172
		350	.220		
		340	.232		
		332	.238		
		360	.182		
		360	.182		
		360	.179		
		360	.182		